Biosensors and Bioelectronics 87 (2017) 320–324

Contents lists available at ScienceDirect

Biosensors and Bioelectronics

journal homepage: www.elsevier.com/locate/bios

Label-free ratiometric DNA detection using two kinds of interaction-responsive emission dyes

Yahui Guo [a], Qingmin Chen [a], Yiting Qi [a], Yunfei Xie [a,*], He Qian [a], Weirong Yao [a,*], Renjun Pei [b]

[a] State Key Laboratory of Food Science and Technology, School of Food Science and Technology, Jiangnan University, Wuxi, 214122 China
[b] Suzhou Institute of Nano-Tech and Nano-Bionics, Chinese Academy of Sciences, Suzhou, 215123 China

ARTICLE INFO

Article history:
Received 8 June 2016
Received in revised form
3 August 2016
Accepted 13 August 2016
Available online 13 August 2016

Keywords:
Ratiometric method
Interaction-responsive emission
Label-free
Dual-wavelength signal

ABSTRACT

A novel ratiometric method with label-free and dual-wavelength signal outputs was developed for DNA detection by employing two kinds of structure-specific dyes that characterising interaction-responsive emission property. The ratiometric platform for the fluorescent detection of DNA was based on target-induced structural transformation from stem-loop structure incorporating split G-quadruplex (SISG) to doubule-strand DNA (dsDNA). The SISG conformation will be disrupted upon binding to the target DNA of perfect complementary sequence, resulting in fluorescence decrease at 610 nm as NMM releases from SISG and fluorescence increase at 450 nm as DAPI inserts into the dsDNA. The method demonstrated its simplicity in that it saved the trouble of expensive and cumbersome functionalization process compared with reported ratiometric methods, and that the two dyes could be excited at the same excitation wavelength. More intriguingly, the combinatorial employment of the two kinds of structure-selective dyes demonstrated a result of "heterosis", in that this sensor simultaneously inherits the sensitivity of DAPI-based signal and the selectivity of G4-based signal. Besides that, this proposed biosensor has been successfully applied in serum sample for DNA detection, and provided a simple and sensitive method for potential DNA detection in bioanalysis, food analysis and disease diagnostic.

1. Introduction

Ratiometric assay has aroused intense scholarly interest due to its remarkable performances including low detection limit, wide linear range, good reliability and selectivity. As the two different signal indicators both have response to analytes, ratiometric methods have the advantages to eliminate the negative effect in complex environment and give more precise measurement (Wang et al., 2016). Besides that, the ratio calculation of dual-signal intensities would contribute a better sensitivity compared with single-signal intensity (Xiong et al., 2015). Increasing efforts are being devoted to develop ratiometric sensors for the detection of DNA (Liu et al., 2016), proteins (Chang et al., 2016; Hu et al., 2016) and small compounds (Shamirian et al., 2016; Zhao et al., 2016; Zhu et al., 2016). For instance, Huang et al.(Huang et al., 2015) developed a FRET-based ratiometric fluorescent probe for pH sensing in living cells by employing DNA-modified AuNPs and an DNA probe of i-motif sequence labelled with dual fluorophores. The reported methods bear advantages of high sensitivity, rapid response and enhanced stability, but always suffer from cumbersome and expensive functionalization or labelling procedure.

Label-free biosensors (LFBs), by definition, do not require the labelling of reporter elements (fluorescent, colorimetric or electrochemical) to facilitate measurements, and has become a powerful tool in the hands of biochemical and environmental analysts. DNA fluorescent dyes with interaction-responsive emission (IRE) property have promoted the development of fluorescence biosensors in a versatile and cost-effective way because of separation-circumvented and modification-free advantages. Considerable efforts have been made to develop sensitive and selective LFBs using IRE dyes, such as Chen et al. (2016) developed a label-free fluorescence biosensor for selective detection of NAD^+ based on nuclease-assisted background suppression using the typical IRE dye SYBR green I, a double-strand DNA (dsDNA) intercalator characterising thousand-fold enhancement of intrinsic fluorescence after binding to dsDNA. Jiang et al. (2015) used QATPE, a dye characterising aggregation-induced emission, for label-free and real-time monitoring of rolling circle amplification reaction.

G-quadruplex (G4) is a noncanonical DNA structure formed by stacking of G-quartets, which are assembled with four guanines through Hoogsteen-type base pairing. G4 have been widely used

* Corresponding author.
E-mail addresses: xieyunfei@jiangnan.edu.cn (Y. Xie), yaoweirongcn@jiangnan.edu.cn (W. Yao).

http://dx.doi.org/10.1016/j.bios.2016.08.041
0956-5663/

as signal transducers in LFBs by employing G4-selective binding dyes (both organic and inorganic) or chromogenic DNAzymes (Guo et al., 2016). Our group has devoted continuous efforts to the developing of LFBs using G4-specific dyes, and developed LFBs for the assays of metal ions (Guo et al., 2015a, 2015b; Xu et al., 2015a, 2015b), nucleic acids (Guo et al., 2014a, 2013), protein (Guo et al., 2014b), enzyme activity (Guo et al., 2015c; Zhou et al., 2016, 2015) etc. We have reported a new G4-selective and responsive ligand, riboflavin, the fluorescence of which could be greatly quenched after binding to K^+-stabilized antiparallel G4 (PW17) (Xu et al., 2015c), and developed a new sensor for K^+ detection based on this phenomenon. Wu et al. (2016) synthesized a G4 ligand Bis(methylpiperazinylstyryl)phenanthroline, that showed strong binding affinity to antiparallel G4s and exhibited a fluorescence enhancement up to 150-fold. The good properties made it a promising candidate serving as a label-free signal output for G4-based LFBs.

In the current study two kinds of IRE dyes, G4-specific and dsDNA-inserting, were employed for the development of a novel ratiometric method for DNA detection based on a two-wavelength LFB by using a stem-loop structure incorporating split G4 probe. The two-wavelength LFB changed fluorescence emission from 610 nm to 450 nm following the target-induced structural transformation from G4 structure to dsDNA. More intriguingly, the two-wavelength emission can be excited at the same wavelength. Compared with other ratiometric assay, this DNA biosensor is modification-free, simple and has a rapid response to obtain readout signals.

2. Material and methods

2.1. Materials

Oligonucleotides were obtained from Sangon Biotechnology Co., Ltd. (Shanghai, China). The sequences of the oligomers are listed in Table S1 (supporting information, SI). N-methyl mesoporphyrin IX (NMM), 4,6-diamidino-2-phenylindole (DAPI) and deuterium oxide (D_2O, 99.8%) were purchased from J&K Scientific Ltd., all other chemical reagents were purchased from Sinopharm Chemical Reagent Co. Ltd (China). All solutions were prepared with water purified by a Milli-Q system (Millipore, Bedford, MA, USA) and stored at 4 . Measurements were performed in 20 mM Tris-HCl buffer (pH 7.4, 10 mM KCl, 5 mM $MgCl_2$), unless stated otherwise.

2.2. Apparatus

The concentrations of DNA solutions were accurately quantified by measuring the absorption at 260 nm on an UV–VIS spectrophotometer (UV-1800, SHIMADZU). Fluorescence spectrometer (F-7000, Hitachi) with a Xenon lamp (450 W) excitation source was employed to record fluorescence spectra. Both excitation and emission slits were set at 10 nm. Circular dichroism spectra were collected from 230 to 320 nm using a circular dichroism spectrometer (MOS-450, BioLogic Science Instruments) at 20 with a 1 nm bandwidth. NMR experiments were performed on a Bruker Aduance III 400 MHZ (9.4 T) spectrometer (Bruker, Germany).

2.3. Fluorescence measurements

The SISG probes were diluted to a concentration of 200 nM in Tris-HCl solution and treated with different concentrations of target DNA (0, 0.5, 1, 2, 4, 6, 8, 10, 20, 40, 60, 80, 100, 120, 140 nM). After incubating the mixture for 30 min, the fluorescence emission spectra were recorded from 420 to 650 nm on a fluorescence spectrometer excited at 380 nm. Both excitation and emission slits were set at 10 nm.

2.4. NMR measurements

The SISG probe and Nv-cDNA for NMR experiments were buffered in 100 mM KCl, 10 mM sodium phosphate buffer (pH 7.0), followed by an annealing procedure, and then lyophilized. The lyophilized DNAs were resuspended in D_2O (99.8%) before NMR measurements to reach a DNA concentration of 2.0 mM.

3. Results and discussion

3.1. Principle of operation

NMM (N-methyl mesoporphyrin IX) is an unsymmetrical anionic porphyrin characterized by a pronounced structural selectivity for G4 but not for duplexes, triplexes, or single-stranded DNA forms. The fluorescence of NMM is negligible, but exhibits a $>$20-fold enhancement upon binding to G4s (Arthanari et al., 1998). DAPI (4′,6-diamidino-2-phenylindole) is a widely used fluorescent stain in fluorescence microscopy that can bind strongly to dsDNA and produces more fluorescence (Kapuscinski, 1995). In this work, a novel two-wavelength LFB for fluorescence ratiometric detection of DNA was developed by employing two kinds of IRE nucleic acid dyes, NMM and DAPI. As illustrated in Scheme 1, the DNA probe initially formed a stem-loop structure through self-complementary hybridization with a G4 structure at tail end. The G4 structure was assembled by two split G-rich sequences at the 5′-end and the 3′-end of the stem-loop structure, named stem-loop structure incorporating split G-quadruplex (SISG) probe. In the absence of target DNA, there was an enhanced fluorescence intensity of NMM because of its specific binding to the split G4 structure at the tail end of the SISG probe. In the presence of target DNA, it hybridized with the loop region of the SISG probe, resulted in formation of dsDNA and disassembly of split G4 structure. As a consequence, NMM would be released from the G4 structure and DAPI subsequently intercalated into the dsDNA, leading to decreased fluorescence intensity of NMM and increased fluorescence intensity of DAPI.

The structural transformation process was validated by the circular dichroism (CD) spectra, which can sensitively reflect conformational changes in the secondary structure of DNA. As shown in Fig. S2 (SI), the positive peak at 290 nm and negative peak at 260 nm indicated the formation of the anti-parallel G4 structure (Sun et al., 2016). When target DNA challenged with SISG probe, the characteristic peaks were displaced by a positive peak at 275 nm and negative peak at 245 nm, which is characteristic of dsDNA in the right-handed B form (Farajzadeh Dehkordi et al.,

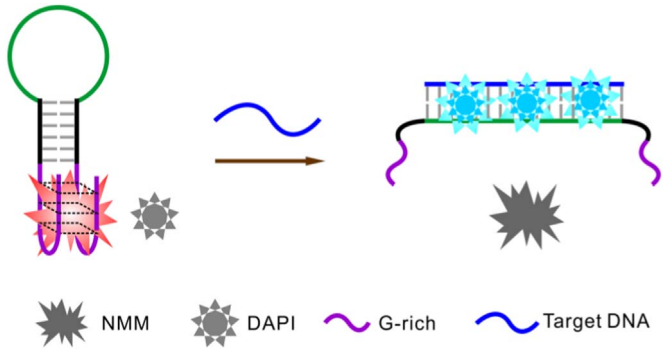

Scheme 1. Schematic illustration of the ratiometric dual-emission biosensor for label-free detection of DNA. The presence of target DNA will disrupt the split G4 structure through hybridizing with the loop region of the SISG probe.

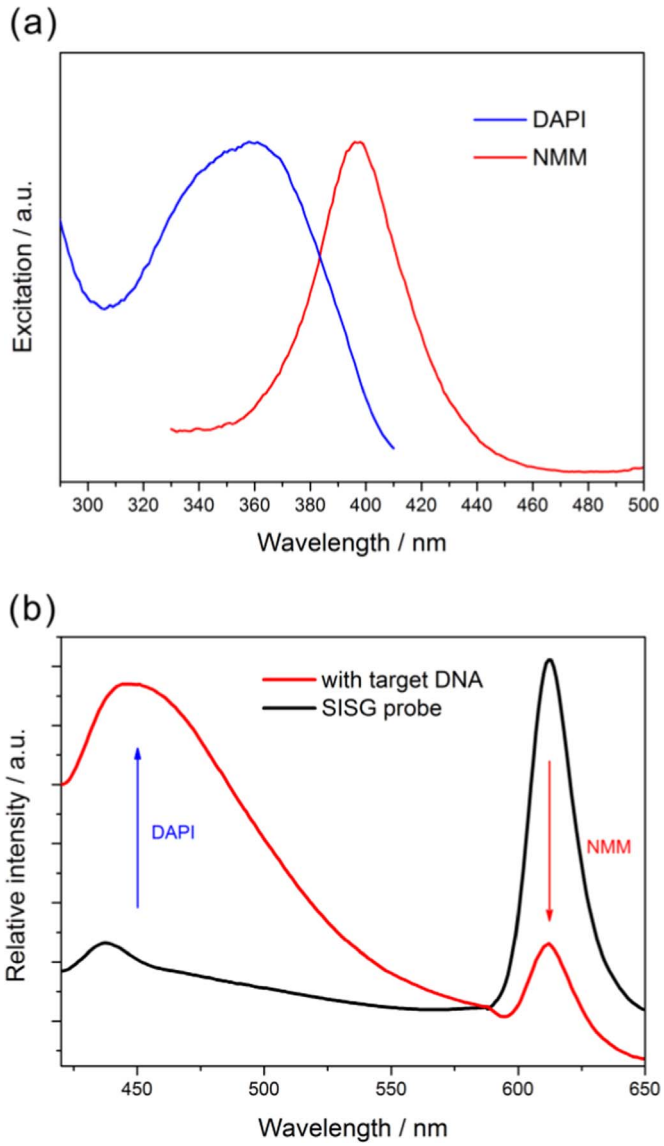

Fig. 1. (a) Photoexcitation spectra of DAPI (40 nM) and NMM (250 nM) in the presence of dsDNA (200 nM SISG +200 nM target DNA) and G4 DNA (200 nM SISG probe), respectively. (b) Fluorescence spectra of the biosensor (200 nM SISG probe +40 nM DAPI +250 nM NMM) in the absence (black line) and presence (red line) of 200 nM target DNA, excited at 380 nm. (For interpretation of the references to color in this figure legend, the reader is referred to the web version of this article.)

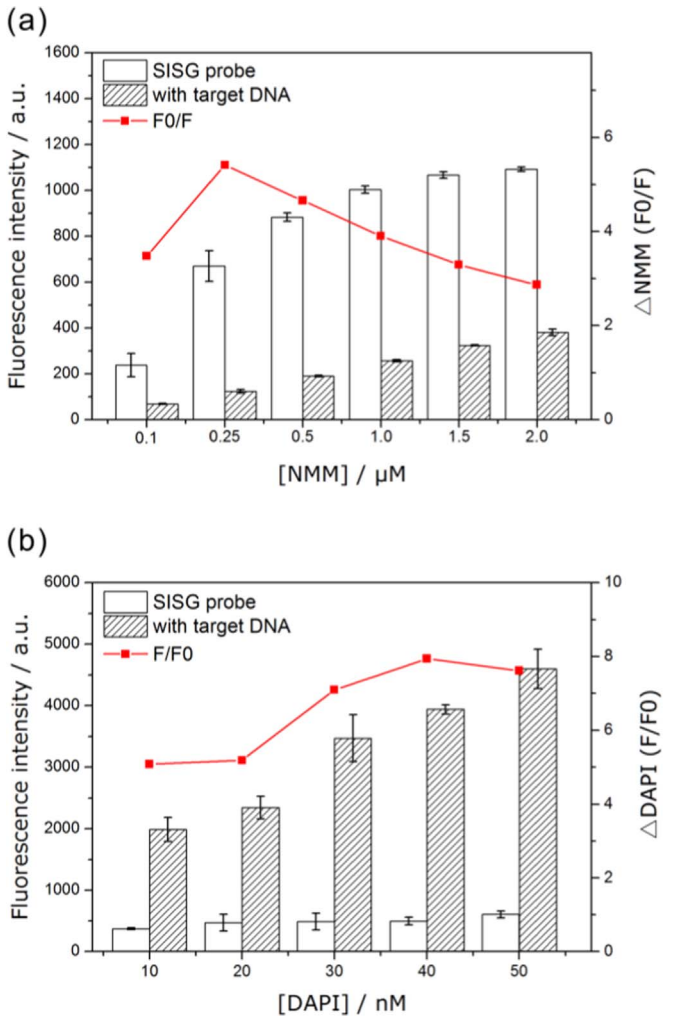

Fig. 2. Fluorescence intensity as a function of the concentration of NMM (a) and DAPI (b) in the absence and presence of 200 nM target DNA respectively.

2015). Besides CD, nuclear magnetic resonance (NMR) measurements have also been widely used to study the solution structure of G4 (Wang and Patel, 1993). One dimension imino proton NMR spectra were recorded in the absence and presence of target DNA respectively. As shown in Fig. S3 (SI), the imino protons between 11 and 12 ppm verified the formation of G4 structure (Phan and Patel, 2003; Wang et al., 1991). After addition of target DNA, the formation of dsDNA resulted in disruption of G4 structure and disappearance of the characteristic peaks from 11 to 12 ppm.

As described above, it was the structural preference of the two IRE dyes that made the rational design feasible for developing the ratiometric DNA sensor. More intriguingly, the two different kinds of dyes, DAPI and NMM, can be excited at the same wavelength. As shown in Fig. S1 (SI), the absorption spectra of NMM and DAPI were overlapped closely in the wavelength band of 300–450 nm. Photoexcitation spectra (Fig. 1a) were also recorded and indicated that the maximum excitation wavelengths of DAPI and NMM were 360 nm and 399 nm respectively. As shown in Fig. 1b, the two dyes exhibited completely separate peaks when simultaneously excited at the wavelength 380 nm (median of their maximum excitation wavelengths). When excited at 380 nm, there was a maximum fluorescence intensity of NMM at 610 nm in the absence of target DNA, on account of the formation of the split G4 structure. After addition of target DNA, it hybridized with SISG probe and opened the stem-loop structure, resulting in disruption of the split G4 structure and formation of dsDNA, consequently generating an enhanced fluorescence intensity of DAPI at 450 nm and a decreased fluorescence intensity of NMM at 610 nm.

3.2. Selection of optimal concentrations of two dyes

In this ratiometric assay, the reverse transcription cDNA of the AU-rich fragment in *Norovirus* RNA sequence (Table S1, SI) was chosen as target DNA (short for NV-cDNA). The NV-cDNA was AT-rich since that DAPI preferably bind to AT-rich region in dsDNA. Before studying the linear response of the two-wavelength LFB to NV-cDNA, the optimal concentrations of NMM and DAPI were investigated firstly. As shown in Fig. 2, the fluorescence intensities in the absence and presence of NV-cDNA were recorded as a function of NMM/DAPI concentration to get a most signal-to-background (S/B) ratio. The S/B ratio is the best when employing 250 nM NMM and 40 nM DAPI in the sensing system. The fluorescence signals toward different concentrations of NV-cDNA were measured under the optimal conditions.

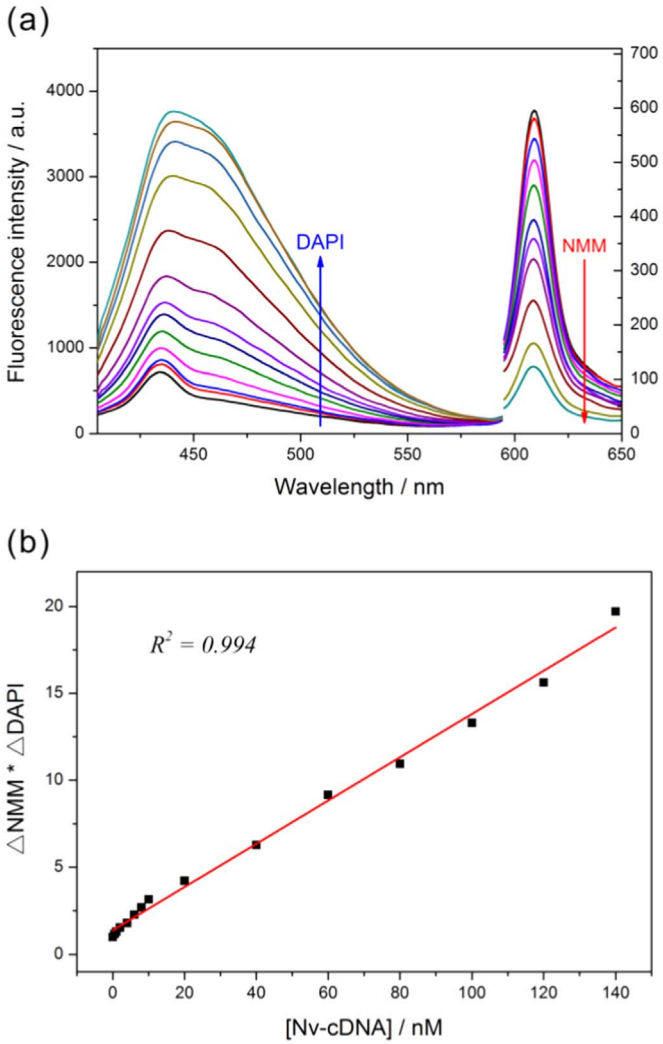

Fig. 3. (a) Fluorescence spectra of the sensor in the presence of increasing concentrations of Nv-cDNA (left: 0, 0.5, 1, 2, 4, 6, 8, 10, 20, 40, 60, 80, 100, 120, 140 nM; right: 0, 10, 20, 40, 60, 80, 100, 120, 140, 160, 180 nM). (b) Ratio value of the DNA sensor as a function of the concentration of Nv-cDNA. Herein, ▵NMM represented F0/F at 610 nm, ▵DAPI represented F/F0 at 450 nm; F0 is the initial fluorescence intensity at 610/450 nm; F0 and F represented the average value from triplex fluorescence measurements of blank samples and analytic samples, respectively.

3.3. The linear response of this ratiometric LFB

Fig. 3a showed the scanning fluorescence spectra of the ratiometric LFB in the presence of increasing concentrations of NV-cDNA. It was noted that the fluorescence of NMM decreased and the fluorescence of DAPI increased with the increase of NV-cDNA concentration. The dependence of fluorescence intensity on Nv-cDNA concentration was studied based on the individual NMM or DAPI signal. As shown in Fig. S4 and S5 (SI), the fluorescence intensity of DAPI increases with the increase of the NV-cDNA concentration in the range of from 0.5 nM to 140 nM; the fluorescence intensity of NMM increases with the increase of the NV-cDNA concentration in the range of 10 nM to 140 nM. ΔNMM(F0/F) and ΔDAPI(F/F0) are the fold changes of the fluorescence intensity of NMM at 610 nm and DAPI at 450 nm, respectively. As shown in Fig. 3b, the value of ΔNMM*ΔDAPI had linear response toward NV-cDNA over the range from 0.5 nM to 140 nM (R^2=0.994). The detection limit of target DNA was estimated to be 0.29 nM based on 3 s rule (taken to be three-fold standard deviation of the blank solution) (Macdougall and Crummett, 1980). The sensitivity of this ratiometric LFB is better than other single-signal LFBs based on IRE

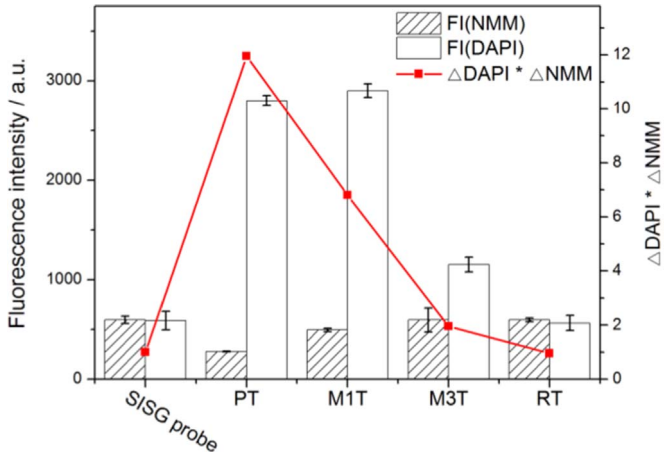

Fig. 4. Selectivity of the ratiometric LFB based on different signal readout modes, FI is short for fluorescence intensity.

(Table S2, SI), of which were at nanomolar level. And comparable to a recently reported two-eimission DNA LFB by using Sc and AR as fluorescence indicators (Fan et al., 2016).

3.4. Selectivity

The selectivity of this proposed ratiometric LFB was evaluated by challenging it with DNA of single-base mismatch sequences (M1T), three-base mismatch sequences (M3T) and random non-complementary sequences (RT) at the same concentration of 100 nM. Fluorescence intensity at individual signal channel was recorded at 610 nm and 450 nm respectively. As shown in Fig. 4, M1T caused significant changes at 450 nm, while the signal change was negligible at 610 nm compared to the perfect-complementary cDNA. Fluorescence intensity changes caused by M3T and RT were not significant compared to the background signal. Compared with single-channel signal, the value of ΔNMM*ΔDAPI (red dots) made it possible to discriminate the mismatched DNA targets more efficiently. This result indicated that this ratiometric LFB had good capacity of discriminating non-perfect complementary sequences.

It's intriguing and inspiring after a comprehensive understanding of sensitivity and selectivity. The quantitation limit is 10 nM when employing NMM alone, while the quantitation range can be extended in the range of 0.5–10 nM after employing DAPI. It was noteworthy that AU-rich sequence of target RNA was selected as the target since DAPI showed binding preference to AT-rich DNA (Schnedl et al., 1977), which will contributed a better S/B ratio. As shown in Fig. S6, a target DNA of random sequence (not AT-rich, RS in Table S1, SI) was aso selected for ratiometric detection based on this two-emission system. Compared with 200 nM Nv-cDNA (AT-rich) with a S/B ratio of ~8, the S/B ration at 450 nm caused by 200 nM RS is less than 3. Thus the employment of dsDNA-binding DAPI improved the sensitivity of this ratiometric LFB. As shown in Fig. 4, the signal caused by the DNA of single-mismatch sequences was comparable to that by the DNA of perfect-complementary sequences when employing DAPI alone, but the employment of G4 structure and G4-binding NMM made it possible to discriminate signal difference. In all, the formation of dsDNA and employment of dsDNA-specific DAPI contributed to a higher sensitivity, and the employment of G4 structure and G4-specific NMM contributed to a better selectivity. The dual-emission ratiometric label-free assay demonstrated an outcome of "heterosis", which bear a combinational property of dual advantages based on target-induced structural transformation and two kinds of structure-specific dyes.

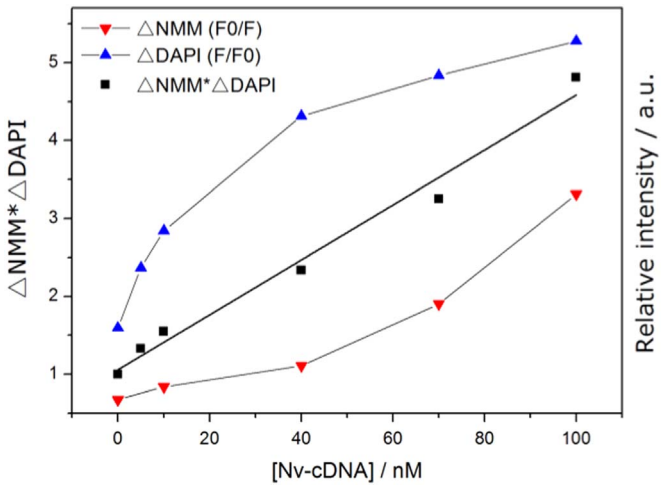

Fig. 5. Fluorescence response of this ratiometric LFB as a function of concentration of Nv-cDNA in diluted serum samples.

3.5. Real sample analysis

As shown in Fig. 5, the meaningful determination of Nv-cDNA was conducted in serum to evaluate the applicability of the developed ratiometric label-free method. Nv-cDNA of different concentration was added in 100-fold diluted serum sample solutions following the same measure procedure. The serum matrix brought high background in NMM and DAPI-based fluorescence signals, which might be due to the interaction between fluorescent dyes and serum components such as polypeptides and proteins (Guo et al., 2013; Ren et al., 2011). Although the serum had a strong influence on the signal intensity of NMM, the combinational signal of NMM and DAPI (ΔNMM*ΔDAPI) still could linearly response to target Nv-cDNA (R^2=0.979), demonstrated better reliability compared with single-signal methods.

To extend the application of this proposed ratiometric method, an AT-rich cDNA of hepatitis A virus RNA (HAV-cDNA, Table S1 in SI) was selected as the target DNA for label-free detection using a customized SISG probe (HAV-probe, Table S1 in SI). As shown in Fig. S7/8/9 (SI), the recorded fluorescence spectra and intensities shown good correspondence to the increasing concentrations of HAV-cDNA. And there was a good linear correlation (R^2=0.993) between ΔNMM*ΔDAPI and concentration of HAV-cDNA over the range of 0.5–90 nM.

4. Conclusions

In the present work, a novel, simple, sensitive and selective ratiometric method was developed for the label-free detection of nucleic acids based on target-induced structural transform strategy using two kinds of structure-selective and interaction-responsive fluorescent dyes, NMM and DAPI respectively. The resulting ratiometric signal was quantitatively correlated to the concentration of Nv-cDNA, and as low as 0.5 nM DNA can be detected without sophisticated design of enzyme-assisted amplifying technology. More intriguingly, the combinatorial employment of the two kinds of structure-selective dyes demonstrated a result of "heterosis", inheriting the sensitivity of DAPI-based assay and the selectivity of G4-based assay. The work enlightened a novel idea of design strategy for label-free ratiometric biosensor based on structure-specific dyes and target-induced structure transformation. Compared with other ratiometric assay, the probe was very simple and elegant. The dyes had a rapid response signal and required less incubation time to obtain read-out signals. This ratiometric LFB was simple, cost-effective and time-saving, also showed potential applications in biomedical analysis.

Acknowledgements

This work was financially supported by National Key Technology R&D Program in the 12th Five year Plan of China (No. 2014BAD04B03, No. 2015BAD16B01), National Natural Science Foundation of China (Nos. 31601552), the Ministry of Science and Technology Major Instrument Science Equipment Development (2012YQ170003) and China Postdoctoral Science Foundation Funded Project (No. 2016M591771).

Appendix A. Supporting information

Supplementary data associated with this article can be found in the online version at doi:10.1016/j.bios.2016.08.041.

References

Arthanari, H., Basu, S., Kawano, T.L., Bolton, P.H., 1998. Nucleic Acids Res. 26, 3724–3728.
Chang, N., Lu, Y., Mao, J., Yang, J., Li, M., Zhang, S., Liu, Y., 2016. Analyst 141, 2046–2052.
Chen, X., Lin, C., Chen, Y., Wang, Y., Chen, X., 2016. Biosens. Bioelectron. 77, 486–490.
Fan, D., Zhu, J., Zhai, Q., Wang, E., Dong, S., 2016. Chem. Commun. 52, 3766–3769.
Farajzadeh Dehkordi, M., Dehghan, G., Mahdavi, M., Hosseinpour Feizi, M.A., 2015. Adv. Pharm. Bull. 5, 477–481.
Guo, Y., Cheng, J., Wang, J., Zhou, X., Hu, J., Pei, R., 2014a. Chem-Asian J. 9, 2397–2401.
Guo, Y., Sun, Y., Shen, X., Chen, X., Yao, W., Xie, Y., Hu, J., Pei, R., 2015a. Anal. Methods 7, 9615–9618.
Guo, Y., Sun, Y., Shen, X., Zhang, K., Hu, J., Pei, R., 2015b. Anal. Sci. 31, 1041–1045.
Guo, Y., Wang, Q., Wang, Z., Chen, X., Xu, L., Hu, J., Pei, R., 2015c. Sens. Actuat. B-Chem. 214, 50–55.
Guo, Y., Xu, P., Hu, H., Zhou, X., Hu, J., 2013. Talanta 114, 138–142.
Guo, Y., Yao, W., Xie, Y., Zhou, X., Hu, J., Pei, R., 2016. Microchim. Acta 183, 21–34.
Guo, Y., Zhou, L., Xu, L., Zhou, X., Hu, J., Pei, R., 2014b. Sci. Rep. 4, 7315.
Hu, Q., Zeng, F., Wu, S., 2016. Biosens. Bioelectron. 79, 776–783.
Huang, J., Ying, L., Yang, X., Yang, Y., Quan, K., Wang, H., Xie, N., Ou, M., Zhou, Q., Wang, K., 2015. Anal. Chem. 87, 8724–8731.
Jiang, H., Zhao, M., Niu, C., Kong, D., 2015. Chem. Commun. 51, 16518–16521.
Kapuscinski, J., 1995. Biotech. Histochem 70, 220–233.
Liu, Y., Ye, M., Ge, Q., Qu, X., Guo, Q., Hu, X., Sun, Q., 2016. Anal. Chem. 88, 1768–1774.
Macdougall, D., Crummett, W.B., 1980. Anal. Chem. 52, 2242–2249.
Phan, A.T., Patel, D.J., 2003. J. Am. Chem. Soc. 125, 15021–15027.
Ren, J., Qin, H., Wang, J., Luedtke, N.W., Wang, E., Wang, J., 2011. Anal. Bioanal. Chem. 399, 2763–2770.
Schnedl, W., Breitenbach, M., Stranzinger, G., 1977. Hum. Genet. 36, 299–305.
Shamirian, A., Samareh Afsari, H., Wu, D., Miller, L.W., Snee, P.T., 2016. Anal. Chem. 88, 6050–6060.
Sun, H.J., Ren, J.S., Qu, X.G., 2016. Acc. Chem. Res. 49, 461–470.
Wang, X., Yu, J., Wu, X., Fu, J., Kang, Q., Shen, D., Li, J., Chen, L., 2016. Biosens. Bioelectron. 81, 438–444.
Wang, Y., de los Santos, C., Gao, X.O., Greene, K., Live, D., Patel, D.J., 1991. J. Mol. Biol. 222, 819–832.
Wang, Y., Patel, D.J., 1993. Structure 1, 263–282.
Wu, S., Wang, L., Zhang, N., Liu, Y., Zheng, W., Chang, A., Wang, F., Li, S., Shangguan, D., 2016. Chemistry 22, 6037–6047.
Xiong, E., Zhang, X., Liu, Y., Zhou, J., Yu, P., Li, X., Chen, J., 2015. Anal. Chem. 87, 7291–7296.
Xu, L., Shen, X., Hong, S., Wang, J., Zhang, Y., Wang, H., Zhang, J., Pei, R., 2015a. Chem. Commun. 51, 8165–8168.
Xu, L., Sun, N., Zhou, L., Chen, X., Wang, J., Wang, Q., Wang, K., Zhang, J., Pei, R., 2015b. Analyst 140, 3352–3355.
Xu, L., Sun, N., Zhou, L., Chen, X., Wang, J., Wang, Q., Wang, K., Zhang, J., Pei, R., 2015c. Analyst 140, 3352–3355.
Zhao, W., Li, Y., Yang, S., Chen, Y., Zheng, J., Liu, C., Qing, Z., Li, J., Yang, R., 2016. Anal. Chem. 88, 4833–4840.
Zhou, L., Cheng, H., Wang, J.E., Pei, R.J., 2016. Chin. J. Anal. Chem. 44, 13–17.
Zhou, L., Shen, X., Sun, N., Wang, K., Zhang, Y., Pei, R., 2015. Analyst 140, 5450–5453.
Zhu, X., Xiao, Y., Jiang, X., Li, J., Qin, H., Huang, H., Zhang, Y., He, X., Wang, K., 2016. Talanta 151, 68–74.